Optimal Transmitter Power Control in Interleave Division Multiple Access (IDMA) Spread Spectrum Uplink Channels*

Zvi Rosberg[1]

(Feb. 8, 2005 ; Revisions: Aug. 17, Nov. 22, 2005, Feb. 07, 2006)

Abstract

The optimal transmitter power control policy in an interleave division multiple access (IDMA) spread spectrum uplink channel is derived. The policy is applied to an IDMA channel with repetition code and a chip-by-chip maximum-likelihood decoder whose sum-rate is compared to the capacity of a linear minimum mean square error multiuser detector and to the Cover-Wyner capacity.

Index Terms

Wireless, Cellular Network, CDMA, IDMA, MMSE, Transmitter Power Control.

I. Introduction

Interleave division multiple access (IDMA) method combined with iterative chip-by-chip (CBC) multiuser detection (MUD) [12] [14] is a relatively new multiple access method for spread spectrum communication. It offers an alternative to the well studied direct sequence code division multiple access (DS-CDMA) method [28] and its respective MUD [25].

Unlike DS-CDMA, where users are spread by different signature codes (which are also used to separate them), IDMA may spread the users with a common sequence code and still enable separation. The separation is made possible by using different interleavers invoked after the spreading.

The spectral efficiency of any multiple access method depends on the code and decoder structures, and on the power control policy. Transmitter power controls for DS-CDMA systems have been studied thoroughly, e.g., [1] [8] [13] [16] [17] [21] [23] [27] [30] [31]. A first study on IDMA power control is given in [15], where the received powers are quantized into discrete values and a linear program is used for optimal power approximation. In this paper, a different optimization approach for IDMA power control is taken revealing the detailed structure of the optimal powers. It worth noting that the objective of the traditional DS-CDMA power controls in the studies above is to achieve signal to interference and noise ratio (SINR) targets before the decoder, whereas the one analyzed here is to achieve SINR targets at the final step of the decoder. Hence, obtaining a direct relation between the controlled powers and the bit error rate (BER).

*This work was partially supported by the City University of Hong Kong, project numbers 7001287 and 7001551.
[1]Zvi Rosberg is with the Department of Communication Systems Engineering, Ben Gurion University, Beer-Sheva, 84105, Israel.

The objective of this study is two-fold: one is to derive the optimal power control for an IDMA channel; the other is to relate the spectral efficiency of IDMA to the Cover-Wyner capacity, on one hand, and to the capacity of the optimally power controlled linear minimum mean square error (MMSE) MUD [18], on the other hand. Comparison to MMSE MUD is chosen since the computational complexity of the optimal MUD increases exponentially with the number of users [25], whereas MMSE MUD has a blind adaptive implementation [10] and attractive computational complexity.

Finding optimal transmission powers involves two sets of controlled variables. One set is the SINR targets and the other is the powers, which are given by a function of the channel gains. It is shown that for a single class of users and practical system parameters and channel gains, the optimal SINR targets are the same for all users and equal the preset lower bound constraint. Moreover, if fading conditions imply that the peak power constraint is inactive, then the optimal powers are given by a channel inversion policy, i.e., powers are set so as to maintain a constant received power. The optimal received power, which is fixed for all users, is derived explicitly and is shown to have a distributed power control policy requiring only channel estimation.

The IDMA-CBC MUD channel model is presented in Section II; its optimal transmitter power control is derived in Section III and its spectral efficiency with repetition code is compared to the Cover-Wyner and the MMSE MUD capacities in Section IV. Finally, conclusions are drawn in Section V.

II. The IDMA-CBC MUD Channel Model

In this study, the IDMA-CBC MUD channel model and its operational principles are confined to a single path synchronous channel and BPSK modulation [14]. A generic transmitter and the IDMA-CBC MUD receiver is illustrated in Figure 1, where the data input train from each user j is denoted by $\{d_j(k)\}$ and the decoded data stream by $\{\hat{d}_j(k)\}$.

Consider J users transmitting trains of binary data over a shared uplink channel using a common spreading sequence, $\mathbf{s} = (s_0, \ldots, s_{N-1}),\ s_n \in \{\pm 1\}$, comprising N chips. The spreading code is immaterial for IDMA. The input data train from each user j, $\{d_j(k)\}$, is encoded by a forward correction code (FEC) and each symbol is spread by $\mathbf{s}$. After spreading a frame of M consecutive equally likely data symbols from each user j, the respective $K = NM$ chips are interleaved by the user dependent permutation π_j. The resulting chip sequence, $\{x_j(k), k = 1, \ldots, K\}$, is then transmitted over the shared uplink channel. Each chip, $x_j(k)$, is related to its corresponding symbol, d, by $x_j(k) = d \cdot s_{mod(\pi^{-1}(k))}$, where $mod(n)$ is n modulo N.

For a synchronous single path channel, it is sufficient to consider only the signals received during a single frame. Assuming ideal squared waveforms for data and chips, the k^{th} received chip in a frame of

an IDMA channel is given by

$$y(k) = \sum_{j=1}^{J} \sqrt{p_j(k)\ h_j(k)}\ x_j(k) + w(k), \quad k = 1, \ldots, K, \tag{1}$$

where $\sqrt{h_j(k)}$ is the random channel gain for user j, $p_j(k)$ is the user transmission power and $w(k)$ is the AWGN background noise with zero mean and power spectral density σ^2.

The IDMA-CBC MUD applies ideas from the seminal work [2] on turbo coding and follows a similar (but not identical) design of soft-input soft-output (SISO) iterative decoding for coded CDMA [29]. As with turbo decoding, IDMA-CBC MUD is an iterative procedure by which two decoding components perform maximum a posteriori (MAP) decoding exchanging extrinsic information during each iteration.

The front-end component of the receiver is a MUD decoder, called Gaussian chip detector (GCD), which receives the initial signal train $\{y(k), k = 1, \ldots, K\}$ and feedback information from J parallel single-user symbol decoders (DECs). The feedback from each DEC in every iteration n is the extrinsic information [2] on the frame chips, $\{x_j(k),\ k = 1, \ldots, K\}$, specified by the logarithmic likelihood ratio (LLR) and denoted by $\{e_j^n(k),\ k = 1, \ldots, K\}$. The LLRs from each DEC j are interleaved by π_j before being delivered to GCD. The extrinsic variable, $e_j^n(k)$, is the information about the k^{th} chip of user j gleaned from the code structure and the prior information about the other chips in the same frame.

The GCD MUD decoder applies the extrinsic information about the chips of all symbols and users for updating the statistics of $\{x_j(k)\}$. The updated statistic for each user j, $\{L_j^n(k)\}$, is then de-interleaved by π_j^{-1} and fed to its corresponding DEC in an LLR form serving as a priori information. Every DEC j decodes the frame symbols of user j based on the code structure and the a priori information. It then extracts the new extrinsic information completing one decoding iteration.

For a large number of users, the multiple access interference (MAI) to every chip is reasonably approximated by a Gaussian distribution. Moreover, interleaving the chips of a large number of symbols, M, makes MAI appear as an additive uncorrelated Gaussian process during every decoding iteration [5]. Consequently, the LLRs exchanged between the GCD and the DECs are sufficient statistics for MAP decoders, which are optimal when the signal is subject to additive uncorrelated Gaussian interference only.

The performance of IDMA-CBC MUD depends on the amount of canceled MAI, equivalently, the amount of variance reduced from the $\{x_j(k),\ \forall\ j, k\}$ variables. For every iteration n, this variance reduction is obtained in the GCD by using all extrinsic variables $\{e_j^n(k), \forall\ j, k\}$. Approximating the MAI to each chip signal with an additive uncorrelated Gaussian process, the extrinsic information about each $x_j(k)$ becomes equivalent to the conditional mean and variance of $x_j(k)$, given $\{e_i^n(l),\ \forall\ i, l\}$. Each DEC

decoder applies these means and variances for adjusting the Gaussian total interference mean and power, respectively, which are then used in the maximum likelihood decoding of each chip.

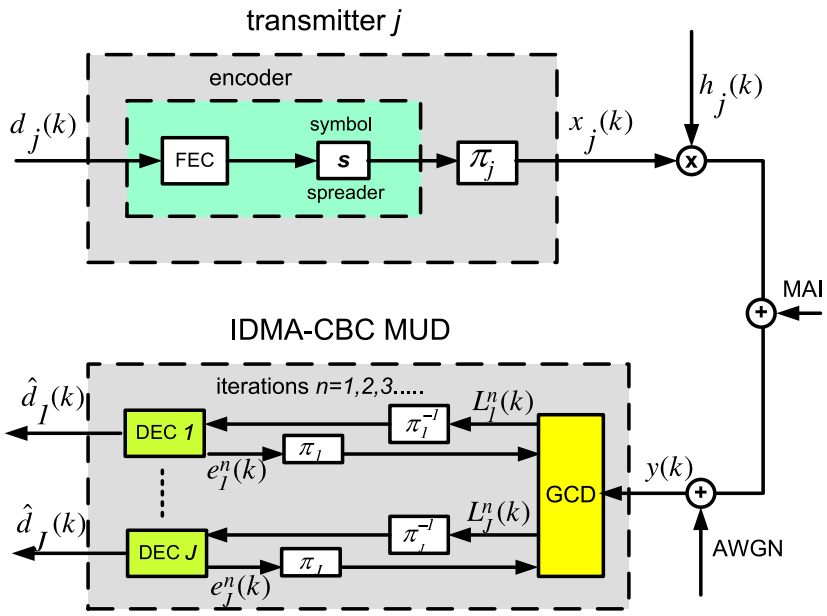

Fig. 1. IDMA-CBC MUD.

Note that with reasonable codes, the conditional variance after every decoding iteration of each chip $x_j(k)$ is reduced. If all variances shrinks to zero, MAI vanishes completely. The amount of reduction depends on the code, the decoder and the received powers $\{p_j(k)h_j(k)\}$.

GCD ignores the code structure [14] and delivers the following LLRs to each DEC j in every iteration n:

$$L_j^n(k) = \log\left(\frac{P\big(y(k)|x_j(k)=+1,\mathcal{F}^{n-1}\big)}{P\big(y(k)|x_j(k)=-1,\mathcal{F}^{n-1}\big)}\right), \quad k=1,\ldots,K, \tag{2}$$

where $\mathcal{F}^{n-1}$ is the σ-algebra induced by $\{y(l),\ \forall\ l\}$ and $\{e_i^{n-1}(l),\ \forall\ i,l\}$.

The LLRs delivered by each DEC j to GCD in iteration n are the following extrinsic variables extracted from the a posteriori probability decoder:

$$e_j^n(k) = \log\left(\frac{P\big(x_j(k)=+1|\mathcal{F}_1^n\big)}{P\big(x_j(k)=-1|\mathcal{F}_1^n\big)}\right), \quad k=1,\ldots,K, \tag{3}$$

where $\mathcal{F}_1^n$ is the σ-algebra induced by $\{L_j^n(l),\ \forall\ l\}$ and the code structure.

The conditional mean and variance of every $x_j(k)$ are derived similarly to the derivation of [29, Eq. (27)] and are given by (see [14, Eqs. (5)–(6)])

$$E\big(x_j(k)|\mathcal{F}_1^n\big) = \tanh\left(e_j^n(k)/2\right) \quad ; \quad V_j^n(k) \stackrel{def}{=} Var\big(x_j(k)|\mathcal{F}_1^n\big) = 1-\tanh^2\left(e_j^n(k)/2\right). \tag{4}$$

The complete computational procedure of IDMA-CBC MUD is given in [14] and requires channel side information (CSI), i.e., $(h_1, \ldots, h_J)$, which can be replaced with estimators.

Note that each $e_j^n(k)$ is a random variable whose distribution is determined by the σ-algebra $\mathcal{F}_1^n$. For large K and M, simulation observations and analysis [6] reveal that upon iteration convergence, $e_j^n(k)$ is approximated by a Gaussian random variable. The Gaussian mean and variance depend on the code and the decoder structures. The power control problem, defined in the next section, concerns with the decoder performance at the iteration convergence point, where

$$V_j^n(k) \approx V_j \stackrel{def}{=} 1 - \tanh^2\left(\frac{Y_{\gamma_j}}{2}\right), \quad j = 1, \ldots, J, \tag{5}$$

and Y_{γ_j} is a Gaussian random variable whose mean and variance are determined by the SINR of the chip signal, γ_j, at the convergence point. The dependency on k in (5) also disappears since all data symbols are assumed to be independent and identically distributed. As in [19], the latter is implied by (3), (4) and the additive uncorrelated Gaussian process of the MAI.

By (4), V_j is the converging conditional variance of an arbitrary chip from user j at the receiver, which by definition is the conditional interfering power of its signal at the receiver. Thus, the unconditional value of V_j, $E(V_j)$, is the power reduction factor of the interference introduced by user j at the iteration convergence point. Iteration convergence for any received power is implied by the fact that for any realization and every k and j, $E\big(V_j^n(k)\big)$ decreases with n. This *convergence condition* is formally proved in the next section.

Also note, that since chip MAI appears as an additive uncorrelated Gaussian process, the chip error rate of the maximum likelihood estimator of $x_j(k)$ at each iteration n is $Q\left(\sqrt{SINR_j^n(k)}\right)$, where Q is the standard Gaussian complementary distribution function and $SINR_j^n(k)$ is the SINR of the chip signal at iteration n. The values of $\{SINR_j^n(k)\}$ can be controlled by a transmitter power control policy analyzed in the next section.

III. The IDMA Power Control Problem

For every user j, let γ_j and γ_j^s be the SINR targets for a chip and a symbol, respectively, in DEC j upon iteration convergence. Due to code and decoder constraints, $\boldsymbol{\gamma} = (\gamma_1, \ldots, \gamma_J)$ are bounded below by $\underline{\boldsymbol{\gamma}} = (\underline{\gamma}_1, \ldots, \underline{\gamma}_J)$. The role of power control is to adapt the transmission powers to the channel gain variations so as to dominate all SINR targets. Instantaneous transmission powers, $\mathbf{p} = (p_1, \ldots, p_J)$, however, are bounded by peak levels denoted by $\overline{\mathbf{p}} = (\overline{p}_1, \ldots, \overline{p}_J)$, e.g., 1 Watt in DCS 1800 and PCS 1900, and 2 Watt in GSM. Since SINR targets determine the BERs, their relation presents a combined optimization problem over the feasible powers and SINR targets.

The overall objective of the power control is finding the optimal SINR targets, $\boldsymbol{\gamma}$, and minimizing the total instantaneous transmission powers, $\mathbf{p}$, for every constellation of channel gains, $\mathbf{h} = (h_1, \ldots, h_J)$, subject to instantaneous SINR and power constraints. The optimization problem is formulated below.

As mentioned in the introduction, unlike traditional DS-CDMA power controls aiming at SINR targets before the decoder, the IDMA power control is aiming at the SINR targets in the final step of the decoder. A code dependent expression for the latter SINRs and their respective constraints are derived next.

A. Chip SINR Constraint

Suppose that for every user j, the power control can maintain a fixed received power, R_j, during the entire frame, and let $\mathbf{p}$ and $\mathbf{h}$ be the powers and channel gains, respectively. Note that DS-CDMA implementations have demonstrated a power control with 1600 power updates per second, which is based on SINR and channel gain estimators. This rate can maintain a constant received power as long as the channel coherence time is not shorter than 0.625 msec, which is appropriate for vehicles traveling at 100 km/h and bandwidth of 1.25 MHz.

The actual instantaneous SINR of the k^{th} chip signal of user j in DEC j during iteration n, $\Lambda_j^n(k)$, is given by

$$\Lambda_j^n(k) = \frac{p_j h_j}{\sigma^2 + \sum\limits_{i \neq j} p_i h_i E(V_i^n(k))}, \tag{6}$$

where σ^2 is the power spectral density of the AWGN background noise and $V_i^n(k)$ is given by (4).

The power control aims at achieving the SINR targets upon iteration convergence, i.e., when MAI interference is maximally canceled. Thus, by (5), the indices of n and k can be omitted from the right hand side of (6) yielding an actual SINR upon convergence of

$$\Lambda_j \stackrel{def}{=} \frac{p_j h_j}{\sigma^2 + \sum\limits_{i \neq j} p_i h_i E(V_i)}. \tag{7}$$

Consequently, if the SINR targets, $\boldsymbol{\gamma}$, are attained by the transmission power control, the following constraint must be applied at the iteration convergence:

$$\frac{p_j h_j}{\sigma^2 + \sum\limits_{i \neq j} p_i h_i f(\gamma_i)} \geq \gamma_j, \quad j = 1, \ldots, J, \tag{8}$$

where, by (5),

$$f(\gamma_j) \stackrel{def}{=} 1 - E\left[\tanh^2\left(\frac{Y_{\gamma_j}}{2}\right)\right], \quad j = 1, \ldots, J. \tag{9}$$

The function $f(\gamma_i)$ reflects the interference cancelation resulting from the iterative turbo decoder. It is code-dependent, takes values in $(0,1)$, and typically strictly decreasing and convex. Note that constraint (8) is a result of parallel user decoding as opposed to successive user decoding, where different constraints apply.

Generally, $f(\gamma_i)$ does not have an analytical expression and is derived by simulation and curve matching. For BPSK with repetition-code (each bit is replicated N times over the symbol chips), it can be shown (based on [6] [19]) that for large K and M, where chip MAI is approximately Gaussian, Y_{γ_j} is also approximately Gaussian with mean and variance $2(N-1)\gamma_j$ and $4(N-1)\gamma_j$, respectively. The function is depicted in Figure 2.

The f function with a concatenation of a rate-$1/2$ convolutional code with generator polynomials $(23,35)_8$ followed by a rate-$1/8$ repetition code is obtained by simulation and is depicted in [15, Figure 5]. The curve there is plotted in a log scale along the y-axis, which after transformation into a linear scale, exhibits a decreasing convex shape. Since the f function with a repetition code is also depicted there in a log scale [15, Figure 2], one can observe that the f corresponding to the convolutional code decreases much faster than the f corresponding to the repetition code. It should be noted that depicting the analytical graph from Figure 2 in a log scale yields a graph which is the same as the one in [15, Figure 2].

Based on these examples and the interpretation of f, it is expected that the more efficient the code is, the sharper is the decreasing rate of its corresponding f function.

The derivative of the $f(\gamma)$ corresponding to repetition code, which is needed below, is given by

$$\begin{aligned} f'(\gamma) \;&= 1+\left(\tfrac{N-1}{2}+\tfrac{1}{8\gamma^3\pi^2(N-1)^2}\right)E\left[\left(\tanh\left(\tfrac{Y}{2}\right)\right)^2\right] \\ &\quad -E\left[\tfrac{Y^2\left(\tanh\left(\frac{Y}{2}\right)\right)^2}{8(N-1)\gamma^2}\right]. \end{aligned} \tag{10}$$

Since the SINR target constraints in (8) are imposed on $\{\Lambda_j^n(k)\}$ at the iteration convergence, it is shown next that $\{\Lambda_j^n(k)\}$ indeed converges as $n\to\infty$.

Using the f function notation, (6) is translated into

$$\Lambda_j^n(k)=\frac{p_jh_j}{\sigma^2+\sum\limits_{i\neq j}p_ih_if\left(\Lambda_i^n(k)\right)}. \tag{11}$$

Suppose that the power control maintains fixed received powers, $\{p_jh_j\}$, during the decoding of any given frame and let $\mathbf{\Lambda}=\left(\Lambda_1,\ldots,\Lambda_J\right)$ denotes an arbitrary vector of instantaneous SINR values. For every $\mathbf{h}$,

$\mathbf{p}$ and $\mathbf{\Lambda}$, define the transformations

$$T_j(\mathbf{\Lambda}) = \frac{p_j h_j}{\sigma^2 + \sum_{i \neq j} p_i h_i f(\Lambda_i)}, \quad 1 \leq j \leq J, \tag{12}$$

and let $\mathbf{T}(\mathbf{\Lambda}) = \big(T_1(\mathbf{\Lambda}), \ldots, T_J(\mathbf{\Lambda})\big)$.

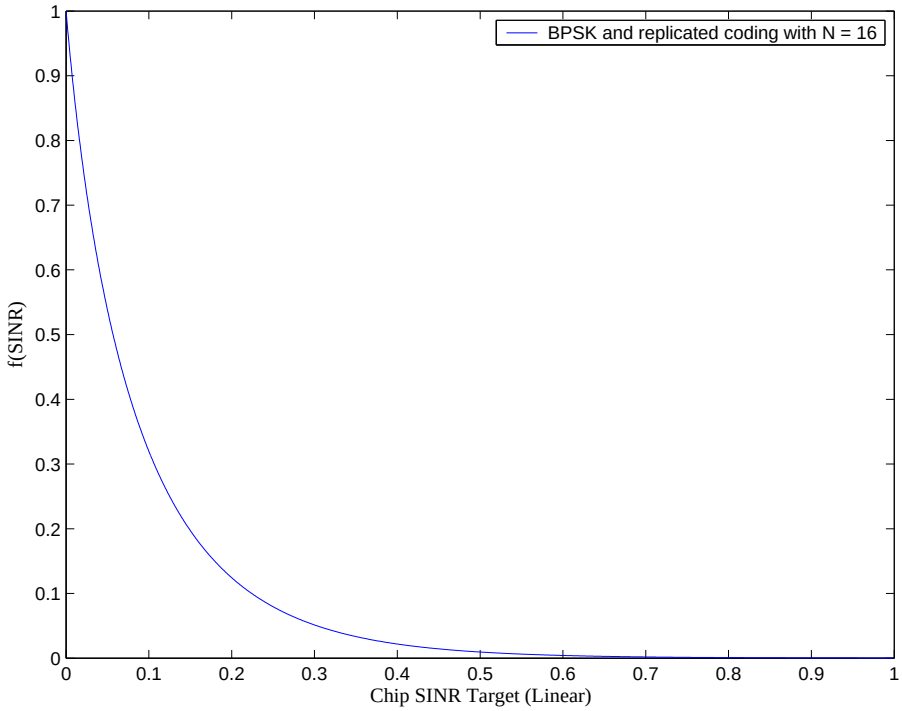

Fig. 2. $f(\gamma)$ vs. chip level SINR in a linear scale.

During the decoding iterations, (11) and (12) imply that the chip SINR values, $\mathbf{\Lambda}^n(k) = (\Lambda_1^n(k), \ldots, \Lambda_J^n(k))$, evolve according to $\Lambda_j^{n+1}(k) = T_j\big(\mathbf{\Lambda}^n(k)\big),\ n \geq 0$, where $\Lambda_j^0(k) = 0,\ \forall\ j, k$, i.e., $f\big(\Lambda_j^0(k)\big) = 1$. Thus, if the sequence $\mathbf{\Lambda}^n(k)$ converges, then it converges to

$$\mathbf{\Lambda}^* = \lim_{n \to \infty} \mathbf{T}(\mathbf{\Lambda}^n(k)). \tag{13}$$

Note that during the iterations $\Lambda_j^{n+1}(k) = T_j\big(\mathbf{\Lambda}^n(k)\big),\ n \geq 0$, the $f(\Lambda_i^n(k))$ function, which reflects the interference cancelation resulting from the iterative turbo decoder, captures the entire information that is relevant for the decoding process.

With a proper decoder, the convergence point is independent of the chip index, k, since all chips are used for decoding the data symbol. To verify convergence, note that $f(\cdot)$ is a positive decreasing function. Thus, starting with $\mathbf{\Lambda}^0 = \mathbf{0}$, $\{\mathbf{T}(\mathbf{\Lambda}^n)\}$ is a monotonically nondecreasing (component-wise) sequence bounded below by $(p_1 h_1, \ldots, p_J h_J)/\sigma^2$. Thus, the limit in (13) exists and $\mathbf{\Lambda}^*$ is the unique fixed point solution to

$$\mathbf{\Lambda} = \mathbf{T}(\mathbf{\Lambda}). \tag{14}$$

The case where all received powers are the same, i.e., $p_j h_j = R,\ \forall\ j$, is of particular interest for the power control problem. For this case, the solution uniqueness and (11) imply that $\mathbf{\Lambda}^* = (\Lambda, \ldots, \Lambda)$, where Λ is the unique solution to

$$\Lambda = \frac{R}{\sigma^2 + (J-1)Rf(\Lambda)}. \tag{15}$$

The bit error rate (BER) of user j is given by $Q\left(\sqrt{\gamma_j^s}\right)$, which is clearly a function of the symbol SINR target, γ_j^s, rather than of the chip SINR target, γ_j. Thus, for BER evaluation, a relation between γ_j^s and γ_j is needed. In the case where $p_j h_j = R, \gamma_j = \gamma,\ \forall\ j$, which is of particular interest for the power control problem, (8) is attained with equality implying that

$$\gamma = \frac{R}{\sigma^2 + (J-1)Rf(\gamma)}. \tag{16}$$

Since the symbol power of each user i is Np_i, the symbol SINR of each user j is given by

$$\gamma_j^s \stackrel{def}{=} \gamma^s = \frac{NR}{\sigma^2 + (J-1)NRf(\gamma)}. \tag{17}$$

By (16) and (17), the required relation is resolved from

$$\frac{1}{\gamma^s} = \frac{1}{\gamma} - \frac{N-1}{N}\frac{\sigma^2}{R}. \tag{18}$$

As observed in the case study below, for practical parameters and optimal powers, $\gamma_j \approx R/\sigma^2$ implying that $\gamma^s \approx \gamma N$.

B. The Optimization Problem

Following the discussion above, the power control with CSI is defined as follows. For every vector of channel gains, $\mathbf{h}$, find:

$$\min_{\boldsymbol{\gamma},\mathbf{p}} \sum_{j=1}^{J} p_j \tag{19}$$

subject to

$$\begin{aligned} &p_j \geq \tfrac{\gamma_j}{h_j}\Big(\sum_{i\neq j} p_i h_i f(\gamma_i) + \sigma^2\Big), \quad 1 \leq j \leq J, \\ &\mathbf{0} \leq \mathbf{p} \leq \overline{\mathbf{p}}, \qquad \boldsymbol{\gamma} \geq \underline{\boldsymbol{\gamma}} \ \ (\text{component wise}). \end{aligned} \tag{20}$$

By (20), for every $\mathbf{h}$ and $\boldsymbol{\gamma}$, the powers are clearly functions of $(\mathbf{h}, \boldsymbol{\gamma})$, i.e., $\mathbf{p} = \mathbf{p}(\mathbf{h}, \boldsymbol{\gamma})$. Since the objective function in (19) is independent of $\boldsymbol{\gamma}$, the problem can be decoupled into two parts. In the first

part, the optimal powers, $\mathbf{p}^*(\mathbf{h}, \boldsymbol{\gamma})$, are derived for any feasible $\boldsymbol{\gamma}$. In the second part, the optimal powers, $\mathbf{p}^*(\mathbf{h})$, are derived by optimizing over all feasible $\boldsymbol{\gamma}$ using the optimal powers, $\mathbf{p}^*(\mathbf{h}, \boldsymbol{\gamma})$, obtained in the first part.

Remark 1: The optimization problem is formulated as centralized problem for a single cell. In practice, interference to the uplink channel from other cells is much smaller compared with interference from the same cell. Therefore, as done in most of the cited papers above, it can either be ignored or added to the background AWGN. Since each base station applies its power control only to its users, the problem setting remains unchanged. This approximation for inter-cell interference is particulary good for a large number of users. Furthermore, although the problem setting is centralized, it is shown that in most practical scenarios the optimal control algorithm can be done distributively.

Remark 2: The power control problem is formulated per chip but the BER will be evaluated per bit by using the relation derived in (18). Also, although we assume that power control maintains fixed received powers during the decoding of any given frame, power updates are not bounded to be at the chip rate. In fact, the power control derived here is applicable only when the channel coherence time is longer than the time interval between feasible power updates. As mentioned above, a feasible update rate of 1600 per second is applicable for vehicles traveling at 100 km/h and using a bandwidth of 1.25 MHz.

C. The Optimal Powers for Given SINR targets

For every vector of SINR targets, $\boldsymbol{\gamma}$, the optimal powers, $\mathbf{p}^*(\boldsymbol{\gamma}, \mathbf{h})$, are explicitly derived as follows. Define the functions

$$I_j^{\boldsymbol{\gamma}}(\mathbf{p}) = \min\left\{\overline{p}_j; \frac{\gamma_j}{h_j}\left(\sum_{i\neq j} p_i h_i f(\gamma_i) + \sigma^2\right)\right\},\ 1 \leq j \leq J, \tag{21}$$

and let $\mathbf{I}^{\boldsymbol{\gamma}}(\mathbf{p}) = \left(I_1^{\boldsymbol{\gamma}}(\mathbf{p}), \ldots, I_J^{\boldsymbol{\gamma}}(\mathbf{p})\right)$.

It is straightforward to verify that for every vector $\boldsymbol{\gamma}$, the vector function $\mathbf{I}^{\gamma}(\mathbf{p})$ is a *standard interference function* [30] implying that the elements of the optimal $\mathbf{p}^*(\boldsymbol{\gamma}, \mathbf{h})$ are given by the unique solution to

$$p_j = \min\left\{\overline{p}_j; \frac{\gamma_j}{h_j}\left(\sum_{i\neq j} p_i h_i f(\gamma_i) + \sigma^2\right)\right\},\quad j = 1, \ldots J. \tag{22}$$

Note that a solution to (22) is of the form $p_j = \frac{\gamma_j}{h_j}\left(\sum_{i\neq j} p_i h_i f(\gamma_i) + \sigma^2\right)$ if and only if the right hand side is less or equals $\overline{p}_j$. This is referred to as the *SINR target condition*, which depends on the optimal $\boldsymbol{\gamma}$ and the channel gain realization, $\mathbf{h}$. If the SINR target condition is not satisfied, a *call outage* occurs. In practice, cell layout design ensures a *fading margin* where call outage is a rare event. Fading

margin can be predetermined since fading distribution must be known upon cell layout. When the SINR target condition is not satisfied for a given $\mathbf{h}$ and some j, it is clearly optimal to set $p_j^*(\mathbf{h}) = 0$. Thus, attention can be restricted to realizations $\mathbf{h}$, where the SINR target condition holds true, i.e., when the peak transmission power constraint is inactive. For convenience, it is also assumed that $\underline{\gamma}_j = \underline{\gamma},\ \forall\ j$. The case with different $\{\underline{\gamma}_j\}$ can be carried through the derivation below with additional minor complexity.

Let $\tilde{f}(\gamma) = \gamma f(\gamma)$ and suppose that

$$\sum_{i=1}^{J} \frac{\tilde{f}(\underline{\gamma}_i)}{1+\tilde{f}(\underline{\gamma}_i)} < 1, \quad \text{i.e.,} \quad \frac{\tilde{f}(\underline{\gamma})}{1+\tilde{f}(\underline{\gamma})} < \frac{1}{J}. \tag{23}$$

Requirement (23) is referred to as the *system feasibility condition* from a reason explained below. For every feasible $\boldsymbol{\gamma}$, it can be verified that if $\sum_{i=1}^{J} \frac{\tilde{f}(\gamma_i)}{1+\tilde{f}(\gamma_i)} < 1$, then the following powers solve (22) without the peak power constraints:

$$p_j^*(\boldsymbol{\gamma}, \mathbf{h}) = \frac{R_j}{h_j}, \quad j = 1, \dots J, \tag{24}$$

where

$$R_j = \frac{\sigma^2 \gamma_j}{\big(1-A\big)\big(1+\tilde{f}(\gamma_j)\big)} \quad \text{and} \quad A = \sum_{i=1}^{J} \frac{\tilde{f}(\gamma_i)}{1+\tilde{f}(\gamma_i)}. \tag{25}$$

That is, for every given SINR targets, $\boldsymbol{\gamma}$, the optimal powers with CSI are given by the *channel inversion* policy in (24)–(25). In practice, the unknown $\mathbf{h}$ are replaced with their estimators. Estimator-based power control and bounds on the optimal values can be derived as in [18].

Since (24) is the unique solution to (22) without the peak power constraints and $p_j^*(\boldsymbol{\gamma}, \mathbf{h})$ must be positive, the condition $A = \sum_{i=1}^{J} \frac{\tilde{f}(\gamma_i)}{1+\tilde{f}(\gamma_i)} < 1$ must hold. As shown below, the latter follows from the *system feasibility condition* in (23).

D. The Optimal SINR targets and Powers

With the explicit solution of $p_j^*(\boldsymbol{\gamma}, \mathbf{h})$, the optimization problem in (19)–(20) can be translated into the following quasiconvex optimization program. First, set the optimal $p_j^*(\boldsymbol{\gamma}, \mathbf{h})$ from (24) in (19)–(20) and define two functions

$$F(x) = (1-x)\tilde{f}^{-1}\Big(\frac{x}{1-x}\Big) \quad \text{and} \quad G(\mathbf{x}) = 1 - \sum_{j=1}^{J} x_j,$$

where $x_j = \tilde{f}(\gamma_j)/\big(1+\tilde{f}(\gamma_j)\big)$ and $\mathbf{x} = (x_1, \dots, x_J)$.

Note that $F(x)$ equals $\frac{\gamma}{1+\tilde{f}(\gamma)}$ after variable substitution implying that $F(x)$ is code dependent. Also, as observed in Figure 3 depicted for repetition code and practical symbol SINR targets greater than 2 dB, $F(x)$ is a strictly convex decreasing function. The $F(x)$ functions corresponding to f functions of other codes, whose decreasing rates are faster than that of the repetition code, would also demonstrate the same structure starting from a point that is even smaller than 2 dB.

By simple algebra, it can be verified that a decreasing $F(x)$ is equivalent to the following: if $\gamma \geq \underline{\gamma}$, then

$$\frac{\tilde{f}(\gamma)}{1+\tilde{f}(\gamma)} \leq \frac{\tilde{f}(\underline{\gamma})}{1+\tilde{f}(\underline{\gamma})}. \tag{26}$$

Consequently, the system feasibility condition (23) implies that for every feasible $\boldsymbol{\gamma}$, $\sum_{i=1}^{J} \frac{\tilde{f}(\gamma_i)}{1+\tilde{f}(\gamma_i)} < 1$. Thus, $\mathbf{p}^*(\boldsymbol{\gamma}, \mathbf{h}) > \mathbf{0}$ and the term "system feasibility condition" is justified.

Assuming the system feasibility condition (23), the optimization problem from (19)–(20) can be now rewritten as

$$\min_{\mathbf{x}} H(\mathbf{x}) \stackrel{def}{=} \frac{\sigma^2 \sum_{j=1}^{J} F(x_j)/h_j}{G(\mathbf{x})} \tag{27}$$

subject to

$$0 < x_j \leq \underline{x} \stackrel{def}{=} \frac{\tilde{f}(\underline{\gamma})}{1+\tilde{f}(\underline{\gamma})},\ j = 1, \ldots, J. \tag{28}$$

Note that (23) implies that $G(\mathbf{x}) > 0$, hence, it is not required to use it as a constraint. Problem (27)–(28) is not necessarily convex. However, since $F(x)$ is convex and $G(\mathbf{x})$ is linear, problem (27)–(28) is a quasiconvex program [4], which is solved by the following sequence of convex separable programs. For every $\lambda \in \Re$, let

$$L_\lambda(\mathbf{x}) = \sigma^2 \sum_{j=1}^{J} \frac{F(x_j)}{h_j} - \lambda G(\mathbf{x}),$$

and consider the problem

$$\min_{\mathbf{x}} L_\lambda(\mathbf{x}) \tag{29}$$

subject to

$$0 < x_j \leq \underline{x},\ j = 1, \ldots, J. \tag{30}$$

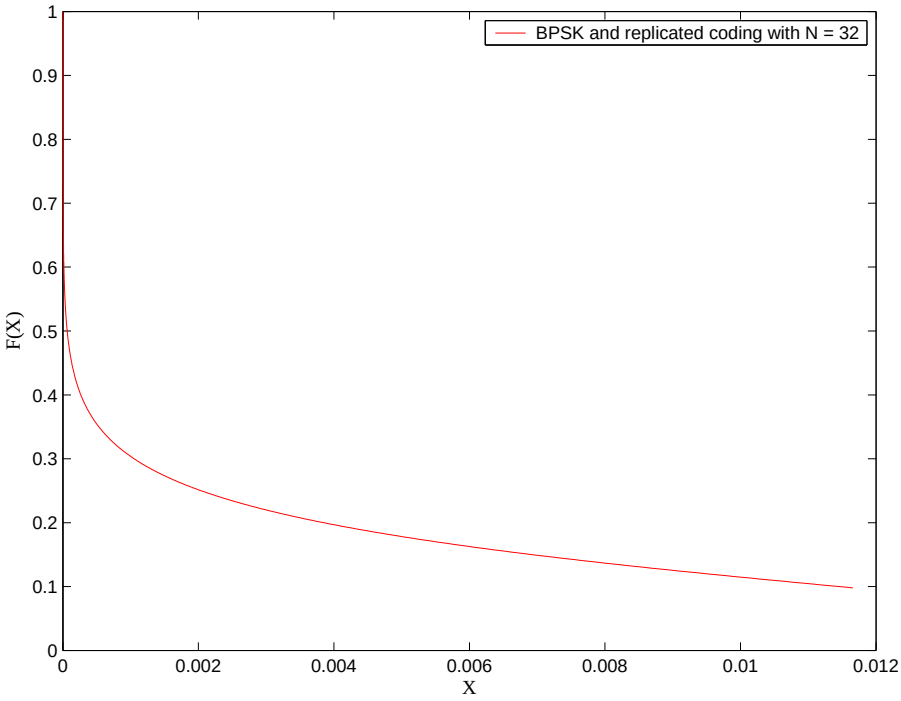

Fig. 3. The $F(x)$ cost function.

For every λ, problem (29)–(30) is a convex program with a strictly convex objective function and therefore having a unique solution, denoted by $\mathbf{x}^*(\lambda)$. Furthermore, $L_\lambda(\mathbf{x})$ is also non-increasing in λ and is greater or equals zero, if and only if

$$\frac{\sigma^2 \sum_{j=1}^{J} F(x_j)/h_j}{G(\mathbf{x})} \geq \lambda, \tag{31}$$

implying that there is a λ^* such that $\mathbf{x}^* \stackrel{def}{=} \mathbf{x}^*(\lambda^*)$ is the solution to both problems, (29)–(30) and (27)–(28), with $L_{\lambda^*}\big(\mathbf{x}^*(\lambda^*)\big) = 0$. Note that λ^* is the minimum value of $H(\mathbf{x})$. The characterization of $\mathbf{x}^*(\lambda)$ and the optimal solution $\mathbf{x}^*$ is derived next.

Invoking the relation $\gamma = \tilde{f}^{-1}\big(x/(1-x)\big)$ implies that

$$\begin{aligned} \frac{dF(x(\gamma))}{dx} &= \frac{1}{(1-x)\tilde{f}'\left(\tilde{f}^{-1}\left(\frac{x}{1-x}\right)\right)} - \tilde{f}^{-1}\left(\frac{x}{1-x}\right) \\ &= \frac{1}{(1-x)\tilde{f}'(\gamma)} - \gamma, \end{aligned}$$

and by the Karush-Kuhn-Tucker (KKT) optimality condition for convex programs [3], $\mathbf{x}^*(\lambda)$ is given by the unique solution to

$$\frac{dF\big(x_j^*(\lambda)\big)}{dx} \begin{cases} \leq -\lambda h_j, & \text{if } x_j^*(\lambda) = \underline{x}, \\ = -\lambda h_j, & \text{if } x_j^*(\lambda) < \underline{x}, \end{cases} \tag{32}$$

where the λ in (32) stands for the λ/σ^2 in (31). Since both variables have the same sign, the results below are not violated by keeping the same notation.

Since $\mathbf{h}$ are sampled from a continuous distribution, no generality is lost by assuming that $h_1 < h_2 < \ldots < h_J$. The fact that $\frac{dF(x_j)}{dx_j}$ is a negative increasing function approaching zero as x approaches one implies that

$$x_j^*(\lambda) = \min\{x_j, \underline{x}\}, \quad \text{where} \quad x_j \quad \text{satisfies} \quad \frac{dF(x_j)}{dx_j} = -\lambda h_j. \tag{33}$$

Furthermore, if $\lambda^* \leq 0$, then $x_j^* = \underline{x}, \ \forall \ j$; and if $\lambda^* > 0$, then $x_{j+1}^* < x_j^*$ for all $x_{j+1}^* \neq \underline{x}$. Note that x_j^* cannot be zero since $F(x_j) \to \infty$ as $x_j \to 0$.

Recalling that $x_j = \tilde{f}(\gamma_j)/(1 + \tilde{f}(\gamma_j))$, the derivation above proves the following theorem.

Theorem 1: Suppose that $h_1 < h_2 < \ldots < h_J$. If $\underline{\gamma}_j = \underline{\gamma}, \ \forall \ j$, the system feasibility condition in (23) holds true and the code has a corresponding strictly convex decreasing function $F(x)$, then the optimal solution to the optimization problem (19)–(20) when the peak transmission power constraint is inactive has the following structure.

(a) There is a threshold index j^* such that

$$\gamma_1^* = \ldots = \gamma_{j^*}^* = \underline{\gamma} < \gamma_{j^*+1}^* < \ldots < \gamma_J^*. \tag{34}$$

Furthermore, for $j > j^*$,

$$\gamma_j^* = \tilde{f}^{-1}\big(x_j^*/(1 - x_j^*)\big), \tag{35}$$

where x_j^* is the unique solution to $\frac{dF(x_j^*)}{dx_j} = h_j \lambda^*$, for some $\lambda^* \geq 0$.

(b) The optimal chip-level transmission powers are given by

$$p_j^* = \frac{R_j}{h_j}, \quad j = 1, \ldots, J,$$

where

$$R_j = \frac{\sigma^2 \gamma_j^*}{\big(1 - A\big)\big(1 + \tilde{f}(\gamma_j^*)\big)} \quad ; \quad A = \sum_{i=1}^{J} \frac{\tilde{f}(\gamma_i^*)}{1 + \tilde{f}(\gamma_i^*)}.$$

■

By the monotonicity of $L_\lambda(\mathbf{x})$ in λ and condition (31), the optimal pair $(\lambda^*, \mathbf{x}^*)$ can be derived using the following bisection algorithm.

Theorem 2: For every $\epsilon > 0$ and initial values $l \leq u$ such that $l \leq H(\mathbf{x}^*) \leq u$, the following bisection algorithm converges to $\mathbf{x}^*$ with an error margin of ϵ.

while ($u - l > \epsilon$**)**

1. $\lambda = (l + u)/2$;
2. Solve the convex program (29)–(30) by computing $\mathbf{x}^*(\lambda)$ in (32);
3. If $L_\lambda\big(\mathbf{x}^*(\lambda)\big) \leq 0$, then set $u = \lambda$; otherwise, set $l = \lambda$.

end

■

The initial interval $[l; u]$ contains the value function $H(\mathbf{x}^*)$. In each iteration, the interval is divided into two, i.e., bisected, so the length of the interval after k iterations is $2^{-k}(u-l)$, where $u-l$ is the length of the initial interval. Thus, exactly $\lceil \log_2((u-l)/\epsilon) \rceil$ iterations are required before the algorithm terminates. Each step involves solving the KKT condition in (32). The length of the interval $[\underline{x}_j^*; \overline{x}_j^*]$ containing each x_j^* at the convergence point is approximately $\frac{\epsilon}{|\frac{\partial H(\mathbf{x}^*)}{\partial x_j}|}$.

E. Discussion

Theorem 1 provides the form of the optimal chip SINR targets and the optimal power control function. It shows that the optimal SINR targets, $\boldsymbol{\gamma}^*$, is a monotonically increasing sequence in the channel gain, where the lower values of the sequence equal the lower bound, $\underline{\gamma}$, on the SINR target. In the two extreme cases, non of the $\boldsymbol{\gamma}^*$ values equal $\underline{\gamma}$ or all of the $\boldsymbol{\gamma}^*$ values equal $\underline{\gamma}$. The theorem also shows that the optimal transmission power of user j, when its channel gain is h_j, is $p_j^* = R_j/h_j$, where $R_j = R_j(f, \sigma^2, \boldsymbol{\gamma}^*)$. The arguments f and σ^2 are known, and $\boldsymbol{\gamma}^*$ is derived by the bisection algorithm given in Theorem 2. From the theorem derivations, it is apparent that Theorem 1 and 2 hold true for any coding scheme, as long as its f function decreases faster than that of the repetition code.

The power control is a distributed channel inversion policy. However, the received signal power for each user j, R_j, is a function of $\boldsymbol{\gamma}^*$, which depends on all channel gains, $\mathbf{h}$. Moreover, in the general case, a bisection algorithm is required for finding them. This would make the power control implementation questionable, unless $\boldsymbol{\gamma}^*$ is independent of the channel gains.

Fortunately, as observed in the case study presented in Section IV and in many other numerical examples with repetition code and practical channel gains (not presented here), the threshold index, j^*, in Theorem 1 equals J. That is, the optimal SINR targets, γ_j^*, are the same for all users and equal the lower bound constraint $\underline{\gamma}$. Consequently, the optimal received powers, $\{R_j\}$, are also the same for all users and the first constraint in (20) is attained with equality. Thus, by equations (15) and (16) in Subsection III-A, the optimal SINR targets and the instantaneous chip SINRs at the iteration convergence point coincide. Since $\underline{\gamma}$ and f are known, the optimal received powers, $\{R_j\}$, are also known. Thus, the optimal power control can be implemented distributively at each user j by constantly estimating its own channel gain h_j.

Applicability of the channel inversion power control may be limited by the channel estimation error. In non-reciprocal channels, channel estimation must be done at receiver and fed back to the transmitter. Thus, estimation error springs from the estimation algorithm and the feedback delay. If the channel varies faster than it can be estimated and fed back to the transmitter, channel inversion power control will perform poorly. However, it has been demonstrated recently that pilot-symbol-based estimation [7] could be quite efficient. For pilot symbol assisted modulation, it has been shown that only a 1-2.5 dB performance degradation compared with perfect channel estimation can be achieved in a flat-fading Rayleigh channel which varies at a rate slower than the symbol rate [20]. For adaptive MQAM modulation using channel estimation based on pilot symbol, only a 1-2.5 dB performance degradation can be achieved for Rayleigh channel [9]. For detecting and decoding turbo coded BPSK signals transmitted over frequency-flat fading channels, estimation error result only in 0.49-1.16 dB performance degradation [24].

Beside the case study presented in Section IV, examples with other values of noise levels, $\sigma^2 = 10^{-8} - 10^{-16}$; spreading code lengths, $N = 8 \times 2^k,\ k = 0, \ldots, 6$; BER $= 10^{-3}, 10^{-4}, 10^{-5}$; lower bounds, $\underline{\gamma} = 2, 3, 4, 5, 6$ dB; and different sampling intervals of the channel gains have been also evaluated. The results for the repetition code are similar to those presented in Section IV.

The reason for having $\gamma_j^* = \underline{\gamma}$ with practical parameters springs from the fact that $f(\gamma)$ decreases with γ sufficiently fast so as sufficient MAI cancelation is attained at the lower bound. Namely, it does not pay off, power-wise, to increase the transmission power any further. From this exact reason, more efficient codes, e.g., the convolution code in Section III-A, where the f function decreases even faster, are expected to produce the same results.

It worth noting that a non-traditional DS-CDMA power control aiming at SINR targets at the final step, rather than at SINR targets before the decoder, would not differ substantially from the IDMA power control and Theorems 1 and 2 can be applied, provided that the respective f function has the required structure.

IV. Capacity Comparison

The potential merit of IDMA is evaluated by comparing its sum-rate with repetition code to the Cover-Wyner capacity, on one hand, and to the capacity of the optimally power controlled DS-CDMA channel with a linear MMSE MUD, on the other hand. The capacity (aka spectral efficiency) is defined as the total number of bits per chip that can be transmitted arbitrarily reliably [26]. Since the bandwidth of a spread-spectrum channel roughly equals the inverse of the chip duration, the capacity can be viewed as the number of bits per second per hertz supported by the system. For a common reference scale, capacities are presented as a function of E_b/N_0, where E_b is the received energy per bit and $N_0 = 2\sigma^2$.

Given a complex-valued channel, the Cover-Wyner capacity for a given E_b/N_0 is resolved from the following equation [26]:

$$C^* = \log_2\Big(1 + C^* \frac{E_b}{N_0}\Big). \tag{36}$$

The DS-CDMA channel capacity with linear MMSE MUD and optimal transmission powers is evaluated as follows. For mathematical tractability, spreading codes are modeled by random sequences and the number of users and the processing gain are assumed to be arbitrarily large [18] [22] [26]. The resulting asymptotic capacity provides excellent approximation for systems with practical processing gains. It also facilitates an analytical closed-form solution for the optimal power control, which is simple to implement [18].

The asymptotically optimal symbol transmission power with multiple user classes, symbol SINR target $\{\underline{\gamma}_i^s\}$ and outage probability $\{\epsilon_i\}$ is derived in [18]. For a single user class with no outage and unbounded transmission power, the optimal symbol transmission power for each user, j, is given by

$$p_j^*(\mathbf{h}) = \frac{\underline{\gamma}^s \sigma^2}{h_j\big(1 - \alpha \frac{\underline{\gamma}^s}{1+\underline{\gamma}^s}\big)}, \quad j = 1, \ldots, J, \tag{37}$$

where $\alpha = J/N$.

Note that the optimal powers are given by a channel inversion policy resulting in a fixed E_b/N_0 for all users and all channel gains. Since $N_0 = 2\sigma^2$ and $E_b = p_j^*(\mathbf{h})h_j$, (37) implies that

$$\frac{E_b}{N_0} = \frac{\underline{\gamma}^s}{2\big(1 - \alpha \frac{\underline{\gamma}^s}{1+\underline{\gamma}^s}\big)}. \tag{38}$$

Given E_b/N_0 and α, the asymptotic MMSE capacity, C^m, is resolved from the following equation [26],

$$C^m = \alpha \log_2\left(1 + \alpha C^m \frac{E_b}{N_0} - \frac{1}{4} F\Big(\alpha C^m \frac{E_b}{N_0}, \alpha\Big)\right), \tag{39}$$

where

$$F(x,y) = \Big(\big(x(1+\sqrt{y})^2 + 1\big)^{\frac{1}{2}} - \big(x(1-\sqrt{y})^2 + 1\big)^{\frac{1}{2}}\Big)^2.$$

The expressions in (37)–(39) specify the MMSE capacity as a function of J/N and E_b/N_0, where the latter is determined by the optimal transmission powers required for attaining a symbol SINR target of $\underline{\gamma}^s$.

Note that the MMSE capacity assumes optimal coding. Thus, the capacity in (39) is an upper bound on the sum-rate of MMSE with any practical coding.

The sum-rate of IDMA with repetition code and optimal power control is evaluated as follows. Since arbitrarily reliable transmission is infeasible with non-optimal coding, the sum-rate is computed for BER of 10^{-4}. As with CDMA-MMSE, the sum-rate with BER of 10^{-4} is also expressed as a function of J/N and E_b/N_0.

By Theorem 1, for every J/N and vector $\boldsymbol{\gamma}$, the optimal chip-level powers are given by

$$p_j^* = \frac{\sigma^2 \gamma_j^* / (1 + f(\gamma_j^*))}{h_j (1 - A)}, \ j = 1, \ldots, J, \tag{40}$$

and the optimal chip level SINR vector, $\boldsymbol{\gamma}^*$, is given by (34)–(35).

Similarly to the optimal power control for CDMA-MMSE, the optimal power control for IDMA is also a channel inversion policy. Unlike with CDMA-MMSE, the bit energy to noise ratios are user dependent, namely

$$\frac{E_b(j)}{N_0} = \frac{\gamma_j^* \big(1 - f(\gamma_j^*)\big)}{2(1 - A)}. \tag{41}$$

For the sake of comparison, the IDMA sum-rate is depicted as a function of the following average bit energy to noise ratio:

$$\frac{E_b}{N_0} = \frac{1}{J N_0} \sum_{j=1}^{J} E_b(j). \tag{42}$$

Given J/N and $\{E_b(j)/N_0\}$, the sum-rate (per chip) of IDMA with complex-valued modulation, R^{idma}, and its corresponding BER are

$$R^{idma} = 2J/N, \qquad BER = \frac{1}{J} \sum_{j=1}^{J} Q\left(\sqrt{\gamma_j^s}\right), \tag{43}$$

where γ_j^s is obtained from $\underline{\gamma_j^*}$ by (18).

Figure 4 depicts the Cover-Wyner upper bound on the multiple access channel capacity, the capacity of MMSE MUD with asymptotically optimal power control and the IDMA sum-rate with repetition code and optimal power control. It is assumed that the noise level is 10^{-9} and the channel gains, $\mathbf{h}$, are uniformly distributed over the unit interval. Although, in practice, gains follow other distributions, e.g., log normal, Rician, Raleigh, the actual distribution is immaterial since the optimal power is a channel inversion policy. The reason for taking a distribution function is to eliminate bias and to cover versatile gain values.

As mentioned above, for many practical system parameters and all E_b/N_0 values, the optimal chip SINR targets turned out to satisfy $\gamma_j^* = \underline{\gamma}, \ \forall \ j$. This can be explained by the sharp decrease of the f

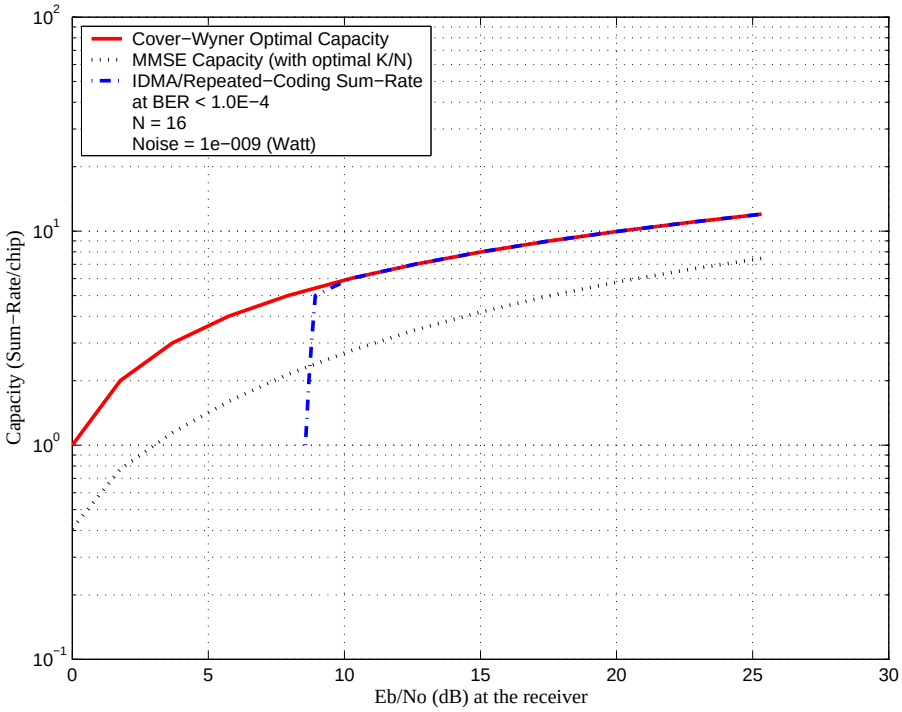

Fig. 4. Sum-Rate and Capacity vs. E_b/N_0.

function (see Figure 2). Furthermore, due to a sharper decreasing rate of the f functions associated with other codes, the same optimal SINR targets are also expected.

Figure 4 illustrates that the IDMA sum-rate is almost the same as the Cover-Wyner capacity for $E_b/N_0 \geq 8.5$ dB. Below 8.5 dB, IDMA with repetition code sharply drops below the MMSE MUD capacity. For more efficient coding, dropping is expected to occur at lower E_b/N_0 values. This dropping is known as the waterfall effect of turbo decoding. Figure 5 reveals that repetition code beyond 16 times deteriorates the performance slightly.

V. Conclusion

In the first part of the paper, the optimal transmitter power control policy was derived for an IDMA spread spectrum uplink channel with iterative turbo MUD. In the second part, it was demonstrated, with the aid of the repetition code, that for practical system parameters the optimal chip SINR targets are the same for all users and equal the lower bound on the SINR targets. The latter observation is of great importance since it enables a simple distributed power control policy.

The optimal IDMA sum-rate with repetition code was also compared with the Cover-Wyner upper bound and with the capacity of the linear MMSE MUD. It was shown that for $E_b/N_0 \geq 8.5$ dB, IDMA sum-rate almost follows the Cover-Wyner upper bound. Below 8.5 dB, IDMA with repetition code sharply drops below the MMSE MUD capacity. For more efficient codes, it is expected that the sharp dropping would occur at lower E_b/N_0 values.

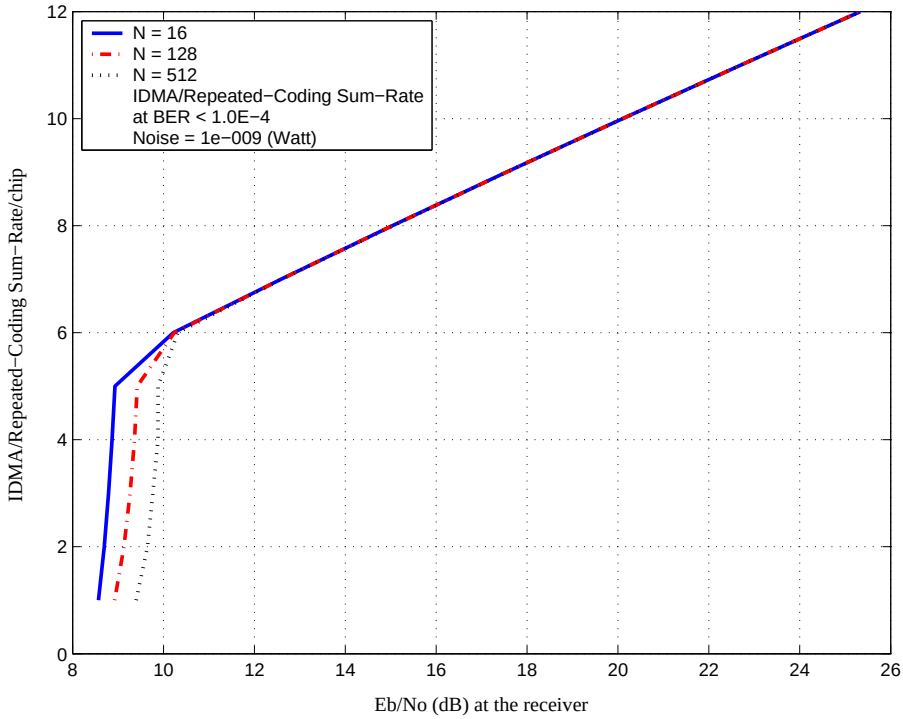

Fig. 5. IDMA Sum-Rate with different symbol lengths vs. E_b/N_0.

ACKNOWLEDGMENT

The author is greatly indebted to Li Ping from the Department of Electronic Engineering, City University of Hong Kong, for introducing me the IDMA power control problem and for utmost important and constructive discussions.

REFERENCES

[1] M. Andersin, Z. Rosberg, and J. Zander, "Distributed Discrete Power Control in Cellular PCS," *Wireless Personal Communications*, vol. 7, pp. 1–21, 1998.

[2] C. Berrou, A. Glavieux, and P. Thitimajshima, "Near Shannon limit error-correction coding and decoding: Turbo codes," Proc. 1993 Int. Conf. on Communications (ICC93), , pp. 10641070, 1993.

[3] D. P. Bertsekas, *Nonlinear Programming*, 2^{nd} edition, Athena Scientific, Mass, USA, ISBN 1-886529-00-0, 2003.

[4] S. Boyd and L. Vandenberghe, *Convex Programming*, Cambridge University Press, Cambridge, UK, ISBN 0 521 83378 7, 2004.

[5] J. Boutros and G. Caire, "Iterative multiuser joint decoding: unified framework and asymptotic analysis," *IEEE Trans. Inform. Theory*, vol. 48, vo. 7, pp. 1772–1793, July 2002.

[6] S. ten Brink, "Convergence behavior of iteratively decoded parallel concatenated codes," *IEEE Trans. Commun.*, vol. 49, pp. 17271737, Oct. 2001.

[7] J. K. Cavers, "An analysis of pilot symbol assisted modulation for Rayleigh fading channels," *IEEE Trans. Veh. Technol.*, pp. 686–693, Nov. 1991.

[8] G. J. Foschini and Z. Miljanic, "A Simple Distributed Autonomous Power Control Algorithm and its Convergence," *IEEE Trans. on Veh. Tech.*, vol. 42, no. 4, pp. 641–646, 1993.

[9] A. J. Goldsmith and S-G Chua, ”Variable-Rate Variable-Power MQAM for Fading Channels,” *IEEE Trans. Commun.*, vol. 45, no. 10, pp. 1218–1230, Oct. 1997.

[10] M. Honig, U. Madhow and S. Verdu, ”Blind Adaptive Multiuser Detection,” *IEEE Trans. Inform. Theory*, vol. 41, no. 4, pp. 944960, July 1995.

[11] W. K. Leung, Lihai Liu and Li Ping, ”Interleaving-based multiple access and iterative chip-by-chip multi-user detection,” *IEICE Trans. on Commun.*, vol. E86-B, pp. 3634-3637, Dec. 2003.

[12] R. H. Mahadevappa and J. G. Proakis, ”Mitigating multiple access interference and intersymbol Interference in uncoded CDMA systems with chip-level interleaving,” *IEEE Trans. Wireless Commun.*, vol. 1, pp. 781792, Oct. 2002.

[13] H. J. Meyerhoff, ”Methods for Computing the Optimum Power Balance in Multibeam Satellite,” *Comsat Tech. Rev.*, vol. 4, vo. 1, 1974.

[14] L. Ping, L. Liu, K.Y. Wu and W. K. Leung, ”A unified approach to multiuser detection and space-time coding with low complexity and nearly optimal performance,” 40th Allerton Conference, Allerton House, USA, pp. 170-179, Oct 2002.

[15] Li Ping and Lihai Liu, ”Analysis and Design of IDMA Systems Based on SNR Evolution and Power Allocation,” Proceeding of VTC 2004-Fall, Los Angeles, CA., vol. 2, pp. 1068-1072, Sept. 2004.

[16] Z. Rosberg, ”Fast Power Control in Cellular Networks Based on Short-Term Correlation of Rayleigh Fading,” Proc. 6th WINLAB Workshop, March 1997, Rutgers University, N.J., 159-182. (Also in the book Advances in Wireless Communications, The Kluwer International Series in Engineering and Computer Science, Edited by J.M. Holtzman and M. Zorzi, pp. 203–217, 1998.)

[17] Z. Rosberg, ”Transmitter Power Control with Adaptive Safety Margins Based on Duration Outage,” *Wireless Personal Communications*, vol. 19, no. 1, pp. 81–90, 2001.

[18] Z. Rosberg, ”Asymptotically Optimal Power Control Policies for MMSE Multiuser Detector,” *ACM Journal of Wireless Networks*, vol. 11, pp. 1–12, 2005.

[19] Z. Shi and C. Schlegel, ”Joint decoding of serially concatenated coded CDMA: iterative schedule study,” Proc. IEEE Information Theory Workshop 2001, Cairns, September 2001.

[20] X. Tang, M-S Alouini and A. J. Goldsmith, ”Effect of Channel Estimation Error on M-QAM BER Performance in Rayleigh Fading,” *IEEE Trans. Commun.*, vol. 47, no. 12, pp. 1856–1864, Dec. 1999.

[21] D. N. Tse and S. V. Hanly, ”Multiaccess Fading Channels Part II: Delay-Limited Capacitis,” *IEEE Trans. Inform. Theory*, vol. 44, no. 7, pp. 2816-2831, 1998.

[22] D. Tse and S. Hanly, ”Linear multiuser receivers: Effective interference, effective bandwidth and user capacity,” *IEEE Trans. Inform. Theory*, vol. 45, pp. 641-657, Mar. 1999.

[23] S. Ulukus and R. D. Yates, ”Adaptive Power Control and MMSE Interference Suppression,” *ACM Journal of Wireless Networks*, vol. 4 no. 6, pp. 489-496, Nov. 1998.

[24] M. C. Valenti and B. D. Woerner, ”Iterative Channel Estimation and Decoding of Pilot Symbol Assisted Turbo Codes Over Flat-Fading Channels,” *IEEE Journal on Selected Areas in Commun.* , vol. 19, no. 9, pp. 1697– 1705, Sept. 2001.

[25] S. Verdu, *Multiuser Detection*. Cambridge, U.K.: Cambridge Univ. Press, 1998.

[26] S. Verdu and S. Shamai, ”Spectral efficiency of CDMA with random spreading,” *IEEE Trans. Inform. Theory*, vol. 45, pp. 622-640, Mar. 1999.

[27] P. Viswanath, D. N. C. Tse, and V. Anantharam, ”Asymptotically Optimal Water-Filling in Vector Multiple-Access Channels,” *IEEE Trans. Inform. Theory*, vol. 47, no. 1, pp. 241-267, 2001.

[28] A. J. Viterbi, *CDMA: Principles of Spread Spectrum Communication*, Addison Wesley Publishing, ISBN 0201633744, May 1995.

[29] X. Wang and H. V. Poor, ”Iterative (turbo) soft interference cancellation and decoding for coded CDMA,” *IEEE Trans. Commun.*, vol. 47, pp. 10461061, July 1999.

[30] R. Yates, ”A Framework for Uplink Power Control in Cellular Radio Systems,” *IEEE JSAC*, vol. 13, no. 7, pp. 1341–1348, Sept. 1995.

[31] J. Zander, ”Distributed Cochannel Interference Control in Cellular Radio Systems,” *IEEE Trans. on Veh. Tech.*, vol. 41, vo. 3, pp. 305–311 1992.